

Structure-Preserving Transformers for Learning Parametrized Hamiltonian Systems

Benedikt Brantner^{*1}, Guillaume de Romemont^{2,3}, Michael Kraus¹, and Zeyuan Li⁴

¹*Max-Planck-Institut für Plasmaphysik, Boltzmannstraße 2, 85748 Garching*

²*DAAA, ONERA, Université Paris Saclay, F-92322, Châtillon, France*

³*Arts et Métiers Institute of Technology, Paris, France*

⁴*Zentrum Mathematik, Technische Universität München, Boltzmannstraße 3, 85748 Garching, Germany*

December 19, 2023

Abstract

Two of the many trends in neural network research of the past few years have been (i) the learning of dynamical systems, especially with recurrent neural networks such as long short-term memory networks (LSTMs) and (ii) the introduction of transformer neural networks for natural language processing (NLP) tasks. Both of these trends have created enormous amounts of traction, particularly the second one: transformer networks now dominate the field of NLP.

Even though some work has been performed on the intersection of these two trends, this work was largely limited to using the vanilla transformer directly without adjusting its architecture for the setting of a physical system.

In this work we use a transformer-inspired neural network to learn a complicated non-linear dynamical system and furthermore (for the first time) imbue it with structure-preserving properties to improve long-term stability. This is shown to be extremely important when applying the neural network to real world applications.

Keywords: Reduced-Order Modeling, Hyper Reduction, Machine Learning, Transformers, Neural Networks, Hamiltonian, Symplectic, Structure-Preserving, Multi-Step Methods

MSC 2020: 68T07, 65D30, 37M15, 65P10

^{*}benedikt.brantner@ipp.mpg.de; Corresponding author.

Introduction

This work addresses a problem in scientific machine learning [2] whose motivation comes from two trends and one observation:

The first trend is using neural networks to identify dynamics of models for which data are available, but the underlying differential equation is either (i) not known or (ii) too expensive to solve. The first problem (i) often occurs when dealing with experimental data (see [8, 14]); the second one (ii) is crucial in *reduced-order modeling* (this will be elaborated on below).

The second trend is a gradual replacement of hitherto established neural network architectures by transformer neural networks; the neural networks that are replaced are primarily recurrent neural networks such as long short-term memory networks (LSTMs, see [19]) that treat time series data, but also convolutional neural networks (CNNs) for image recognition (see [10]).

The observation mentioned at the beginning of this section is the importance of including information about the physical system into a machine learning model. In this paper the physical property we consider is *symplecticity* (see [1, 3, 16, 27]). There are essentially two approaches through which this property can be considered: the first one is the inclusion of terms in the loss function that penalize non-physical behaviour; these neural networks are known as physics-informed neural network (PINNs¹, see [30]). The other approach, and the one taken here, is to hard-code physical properties into the network architecture; the best example of this are “symplectic neural networks” (SympNets, see [21]).

As a motivational example where all of these trends and observations come into play, we consider *Reduced-order modeling* (see [26, 25, 13]). For this we have the following setting: Suppose we are given a high-dimensional parametric ordinary differential equation (PODE), also referred to as the full order model (FOM), obtained from discretizing a parametric partial differential equation (PPDE). Typically we have to solve the high-dimensional PODE for many different parameter instances (see [25, 13]), resulting in prohibitively expensive computational costs.

In order to alleviate the computational cost involved in solving the high-dimensional PODE many times, reduced-order modeling builds a reduced model based on training data. A typical reduced-order modeling framework consists of three stages:

1. solving the FOM for some parameter instances to obtain *training data*.
2. constructing two maps, called *reduction* and *reconstruction*, that map from the FOM space to a space of much smaller dimension and from this smaller space to the FOM space respectively. This is referred to as the *offline stage*.
3. solving the reduced model. This is a PODE of much smaller dimension. This step is referred as the *online stage*.

This work addresses the third step in this framework, the *online stage*, with a method inspired by the two trends and the observation mentioned above. Efforts to use neural networks for the online stage² have been made by other authors; the approaches presented in [26, 13] use long short-term memory (LSTM, [19]) networks for this step for example.³ Above we described the gradual replacement of LSTMs by transformers as the second trend; we also aim to do this here.

We should note that transformer neural networks have also been used for the online stage in reduced order modeling, notably in [18, 32], but in these cases the vanilla transformer was applied without taking physical properties of the system into account, which means that these approaches do not fall into one category with e.g. SympNets. Motivated by reduced-order modeling for Hamiltonian systems (see [28, 33, 6]) this work aims at imbuing a transformer with structure-preserving properties (i.e. symplecticity) to be applied to a parametric Hamiltonian system.

The rest of this paper is structured as follows: in section 1 we introduce basic notions of Hamiltonian systems that we use to describe our particular physical system. In sections 2 and 3 we introduce transformer neural networks and symplectic neural networks (SympNets) respectively. In section 4 we describe the novel architecture (structure-preserving transformers) and in section 5 we demonstrate its efficacy.

¹See [6] for an application of PiNNs that considers symplecticity.

²The offline stage of reduced order modeling for Hamiltonian systems is discussed in [28, 33, 5].

³Apart from neural networks, there are also other approaches to alleviate the cost during the online stage, notably the “discrete empirical interpolation method” (DEIM, [7]).

1 Hamiltonian Systems

Different mechanical systems allow for different mathematical descriptions. If one deals with conservative systems (i.e. non-dissipative ones) then the canonical choices are the ‘‘Lagrangian’’ and the ‘‘Hamiltonian’’ formalism (see [1, 16, 27]). In this work we will exclusively focus on the Hamiltonian formalism, which is outlined in this section.

For the purposes of this work we focus on *Hamiltonian systems in canonical coordinates*⁴ which are defined on even-dimensional vector spaces \mathbb{R}^{2d} . In order to define a Hamiltonian system we then need a *Hamiltonian* and a *symplectic structure*.

A *Hamiltonian* is a differentiable function (which we will assume to be smooth) H defined on \mathbb{R}^{2d} , i.e. $H \in C^\infty(\mathbb{R}^{2d}, \mathbb{R})$. As *symplectic structure* we take the canonical one⁵:

$$\mathbb{J} = \begin{pmatrix} \mathbb{O} & \mathbb{I}_d \\ -\mathbb{I}_d & \mathbb{O} \end{pmatrix}. \quad (1)$$

The equations of motion, based on H and \mathbb{J} , are then described through the following vector field:

$$V_H(\mathbf{z}) := \mathbb{J}_d \nabla_{\mathbf{z}} H. \quad (2)$$

The coordinates, called \mathbf{z} above, of a Hamiltonian system are usually split into two parts: $\mathbf{z} = (\mathbf{q}, \mathbf{p})$. Here $\mathbf{q} \in \mathbb{R}^d$ are the first d coordinates and $\mathbf{p} \in \mathbb{R}^d$ are the remaining ones. With this we can rewrite the equations of motion:

$$\begin{aligned} \dot{q}_i &\equiv \frac{d}{dt} q_i = \frac{\partial H}{\partial p_i}, \\ \dot{p}_i &\equiv \frac{d}{dt} p_i = -\frac{\partial H}{\partial q_i}, \quad i = 1, 2, \dots, d. \end{aligned} \quad (3)$$

We further refer to \mathbf{q} as *positions* and \mathbf{p} as *momenta*.

The following gives a very simple example of a Hamiltonian system:

Example 1. For a one-dimensional harmonic oscillator, the Hamiltonian is given by

$$H = \frac{p^2}{2m} + \frac{1}{2}kq^2,$$

and its equations of motion are:

$$\begin{aligned} \dot{q}(t) &= \frac{p(t)}{m}, \\ \dot{p}(t) &= -kq(t). \end{aligned}$$

Remark. Here the Hamiltonian is *separable*, i.e. it can be written as $H(q, p) = T(p) + V(q)$. In this case we refer to T as the *kinetic energy*, to V as the *potential energy* and to H as the total energy of the system.

1.1 Symplectic Transformations

The flow of eq. (3) has a very strong property: it is a symplectic transformation (see [1, 3, 16, 27]). In order to define general symplectic mappings we first define linear ones:

Definition 1. A linear mapping $A : \mathbb{R}^{2d} \rightarrow \mathbb{R}^{2d}$ is called *symplectic* if

$$A^T \mathbb{J}_{2d} A = \mathbb{J}_{2d}.$$

We say that the matrix A preserves the symplectic structure \mathbb{J}_{2d} .

Now we can define *symplecticity for general mappings*:

⁴Hamiltonian systems can analogously be defined on every even-dimensional differential manifold (see [1, 3]).

⁵In principle a symplectic structure on \mathbb{R}^{2d} can be defined through any skew-symmetric non-degenerate matrix. But in this case one can always find a global transformation to a canonical Hamiltonian system for which the symplectic structure is \mathbb{J} .

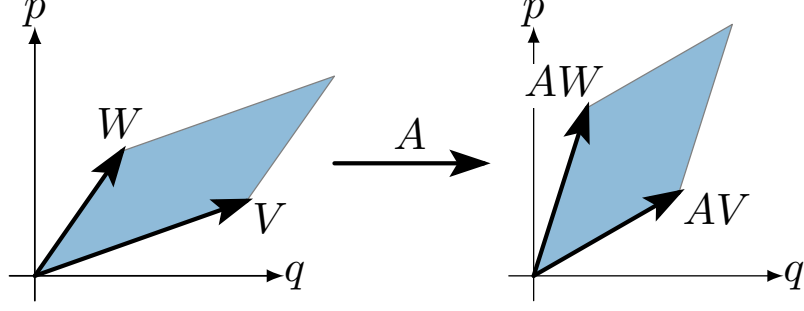


Figure 1: Symplecticity of a linear map A .

Definition 2. A differentiable map $\phi(y) : U \rightarrow \mathbb{R}^{2d}$ (where $U \subset \mathbb{R}^{2d}$ is a open set), is called **symplectic** if the Jacobian matrix $\nabla_y \phi$ is everywhere symplectic, i.e. if $\forall y \in U$:

$$(\nabla_y \phi)^T \mathbb{J}_{2d} (\nabla_y \phi) = \mathbb{J}_{2d}.$$

It can be proved that the exact flow $\varphi_t : (\mathbf{p}(0), \mathbf{q}(0)) \mapsto (\mathbf{p}(t), \mathbf{q}(t))$ of a Hamiltonian system preserves the symplectic structure (see e.g. [16]):

Theorem 1. Let $H(\mathbf{p}, \mathbf{q})$ be a twice continuously differentiable function on $U \subset \mathbb{R}^{2d}$. Then, for each fixed t , the flow φ_t is a symplectic transformation wherever it is defined.

Like any other matrix \mathbb{J}_{2d} is equivalent to a bilinear form on \mathbb{R}^{2d} defined as $\omega : (\mathbf{W}, \mathbf{V}) \mapsto \mathbf{W}^T \mathbb{J}_{2d} \mathbf{V}$ and this bilinear form can be given a geometric interpretation. For this consider a parallelogram in \mathbb{R}^{2d} spanned by two vectors $\mathbf{W} = (\mathbf{W}^q, \mathbf{W}^p)^T = (W_1^q, W_2^q, \dots, W_d^q, W_1^p, W_2^p, \dots, W_d^p)^T \in \mathbb{R}^{2d}$ and $\mathbf{V} = (\mathbf{V}^q, \mathbf{V}^p)^T = (V_1^q, V_2^q, \dots, V_d^q, V_1^p, V_2^p, \dots, V_d^p)^T \in \mathbb{R}^{2d}$:

$$P = \{a\mathbf{W} + b\mathbf{V}, 0 \leq a, b \leq 1\}.$$

then the bilinear form applied to \mathbf{W} and \mathbf{V} is the sum of the oriented areas of the projection of P onto the coordinate planes $(q_i, p_i)_{i=1,2,\dots,d}$:

$$\omega(\mathbf{W}, \mathbf{V}) := \mathbf{W}^T \mathbb{J} \mathbf{V} = \sum_{i=1}^d (W_i^q V_i^p - V_i^q W_i^p) = \sum_{i=1}^d \det \begin{pmatrix} W_i^q & V_i^q \\ W_i^p & V_i^p \end{pmatrix}.$$

Then the symplecticity of a linear mapping means that the sum of oriented areas of the projection of P onto the coordinate planes (q_i, p_i) is the same as that of the transformed parallelogram $A(P)$, i.e.:

$$\omega(\mathbf{W}, \mathbf{V}) = \omega(A\mathbf{W}, A\mathbf{V}).$$

Furthermore symplecticity *implies volume preservation*. If a volume in \mathbb{R}^{2d} is spanned by d vectors $\mathbf{U}_1, \dots, \mathbf{U}_d$, i.e. $\text{vol} = \det([\mathbf{U}_1, \dots, \mathbf{U}_d])$, then it holds that $\text{vol} = \det([A\mathbf{U}_1, \dots, A\mathbf{U}_d])$ for a symplectic linear map A . That this holds can be seen through a Laplace expansion⁶: We can successively delete rows and columns until we end up with an expression that is the sum of terms like $\omega(\mathbf{W}, \mathbf{V})$ which are preserved under a symplectic transformation⁷. In general the following holds:

Theorem 2. Define the volume in phasespace as $\text{vol}(U) = \int_U dy$. Then all linear and nonlinear symplectic mappings are area preserving, i.e., given a symplectic map $\phi(y) : U \rightarrow \mathbb{R}^{2d}$, $\text{vol}(U) = \text{vol}(\phi(U))$.

For a proof see e.g. [16]. Again, all symplectic maps are volume-preserving, but not all volume-preserving mappings are symplectic.

⁶The Laplace expansion (see e.g. [24]) for a determinant says that for $V \in \mathbb{R}^{d \times d}$ it holds that $\det(V) = \sum_{j=1}^d (-1)^{i+j} v_{ij} \det(V_{ij})$. Here V_{ij} is the matrix V from which the i -th row and the j -th column have been deleted.

⁷Note however that volume preservation does not imply symplecticity, the second property is much stronger than the first one.

1.2 Symplectic Integrators

Here we refer to *integrators* as numerical methods that approximate the flow of an ODE φ_t , i.e. they are mappings $\phi : \mathbb{R}^{2d} \rightarrow \mathbb{R}^{2d}$ such that ϕ is in some sense close to φ_h for a fixed time step⁸ h .

Symplecticity is a very strong property that greatly restricts the space of possible mappings and restricting an integrator to those symplectic maps, i.e. requiring $(\nabla\phi)^T \mathbb{J}_{2d} \nabla\phi = \mathbb{J}_{2d}$, has proved very advantageous for a great variety of numerical schemes for solving ODEs (see [16, 27, 33, 23]). Such *symplectic integrators* achieve long-term stability, higher accuracy and (near) conservation of the total energy of a Hamiltonian system.

For integrators (with a fixed time-step length) we distinguish between *one-step* and *multi-step* methods. One-step methods are mappings $\phi : \mathbb{R}^{2d} \rightarrow \mathbb{R}^{2d}$ that aim to approximate the flow of an ODE and take one datum, the current time step, as input. Multi-step methods are mappings $\psi : \times_k \text{times} \mathbb{R}^{2d} \rightarrow \mathbb{R}^{2d}$ that take multiple data as input to produce the next time step. Unlike one-step methods, multi-step methods require another $k - 1$ time steps (or approximations thereof) z_1, \dots, z_{k-1} to start the scheme besides the regular initial condition z_0 .

An well-known example of symplectic one-step integrator is implicit midpoint rule:

$$z_{n+1} \equiv \phi_{\text{mp}}(z_n) = z_n + h \mathbb{J}_{2d} \nabla H \left(\frac{y_{n+1} + y_n}{2} \right). \quad (4)$$

The midpoint rule is easily proven to be symplectic, i.e. $(\nabla_z \phi_{\text{mp}})^T \mathbb{J}_{2d} \nabla_z \phi_{\text{mp}} = \mathbb{J}_{2d}$ (see e.g. [16, 27]). Whereas there exists a broad body of work investigating various one-step methods and their structure-preserving properties, the theory of multi-step methods is less well-established; it is not even straightforward to define a notion of symplecticity for such a method (see e.g. [9, 12]). This will be elaborated on in section 4.

Even though they are less explored, multi-step methods are of great interest for this work. A neural network that could resolve many steps (i.e. that can resolve a time series) can be expected to perform much better than one that only sees one time step at a time.

In order to construct a network that can resolve time series while at the same time also preserve structure, we utilize the transformer architecture.

2 Transformers

The motivation for the transformer architecture (see [34]) came originally from natural language processing (NLP) tasks and it has come to dominate that field⁹. Transformer models are a type of neural network architecture designed to process sequential material, such as sentences or time-series data. The transformer has replaced, or is in the process of replcaing, earlier architectures such as long short term memory (LSTM) networks (see [15]) and other recurrent neural networks (RNNs, see [31]).

The transformer architecture is essentially a combination of an attention layer and a residual net (ResNet¹⁰, see [17]). This architecture is visualized in figure 2.¹¹ The improvements compared to RNNs and LSTMs include the ability to better capture long-range dependencies and contextual information and its near-perfect parallelizability for computation on GPUs and modern hardware.

⁸One can also define integrators for varying step lengths. This is discussed in e.g. [16].

⁹The Transformer is the T in chatGPT and is the key element for generative AI.

¹⁰The simplest form of a ResNet is a regular feedforward neural network with an add connection: $x \rightarrow x + \sigma(Wx + b)$.

¹¹The three arrows going into the multihead attention module symbolize that the input is used three times: twice when computing the correlation matrix C and then again when the input is reweighted based on C . In the NLP literature those inputs are referred to as “queries”, “keys” and “values” (see [34]).

The attention layer, the first part of a transformer layer, takes a series of vectors $z_\mu^{(1)}, \dots, z_\mu^{(T)}$ as input (the μ indicates a specific time sequence) and outputs a *learned convex combination of these vectors*. So for a specific input:

$$\text{input} = [z_\mu^{(1)}, z_\mu^{(2)}, \dots, z_\mu^{(T)}],$$

we get the following for the output of an attention layer:

$$\text{output} = \left[\sum_{i=1}^T y_i^{(1)} z_\mu^{(i)}, \sum_{i=1}^T y_i^{(2)} z_\mu^{(i)}, \dots, \sum_{i=1}^T y_i^{(T)} z_\mu^{(i)} \right]$$

With all the coefficients satisfying $\forall j = 1, \dots, T : \sum_{i=1}^T y_i^{(j)} = 1$. It is important to note that the mapping

$$\text{input} \mapsto \left([y_i^{(j)}]_{i=1, \dots, T, j=1, \dots, T} \right) \quad (5)$$

is nonlinear. These coefficients are computed based on a correlation of the input data and involve learnable parameters that are changed during training.

The correlation in the input data is computed through a *correlation matrix* : $Z \rightarrow Z^T A Z =: C$. The correlations in the input data are therefore determined by computing weighted scalar products of all possible combinations of two input vectors where the weighting is done with A ; any entry of the matrix $c_{ij} = (z_i^{(\mu)})^T A z_j^{(\mu)}$ is the result of computing the scalar product of two input vectors. So any relationship, short-term or long-term, is encoded in this matrix.¹²

In the next step a softmax function is applied column-wise to C and returns the following output:

$$y_i^{(j)} := [\text{softmax}(C)]_{ij} := e^{c_{ij}} / \left(\sum_{i'=1}^T e^{c_{i'j}} \right). \quad (6)$$

This softmax function maps the correlation matrix to the a sequence of *probability vectors*, i.e. vecors in the space $\mathcal{P} := \{\mathbf{y} \in [0, 1]^d : \sum_{i=1}^d y_i = 1\}$. Every one of these d probability vectors is then used to compute a convex combination of the input vectors $[z_\mu^{(1)}, z_\mu^{(2)}, \dots, z_\mu^{(T)}]$, i.e. we get $\sum_{i=1}^T y_i^{(j)} z_\mu^{(i)}$ for $j = 1, \dots, T$.

Remark. Figure 2 indicates the use of a *multi-head attention layer* as opposed to a *single-head attention layer*. What we described in this section is single-head attention. A multi-head attention layer is slightly more complex: it is a concatenation of multiple single-head attention layers. This is useful for NLP tasks¹³ but introduces additional complexity that makes it harder to imbue the multi-head attention layer with structure-preserving properties.

3 Symplectic Neural Networks

The SympNet (see [21] for the eponymous paper) is a neural network architecture that can approximate arbitrary canonical symplectic maps. Each layer of a SympNet only transforms q or p with a map that depends exclusively on the other variable, as described in figure 3. Based on this principle, i.e. only transforming q or p coordinates at one time, it is easy to build neural networks that preserve the symplectic structure.

The most striking theoretical results pertaining to SympNets is that they are, like regular feedforward neural networks (see [20]), “universal approximators”: they can approximate any canonical symplectic map; more concretely set of SympNets is dense (in some topology) in the set of all canonical symplectic maps (see [21]). We will state this theorem more rigorously below.

The original SympNet paper presents two different approaches for building these structure-preserving layers, but we will here only focus on one, the so-called “gradient-type layers”. They have the following

¹²In the *GPT-2 model*, the input sequence is at maximum 1024 tokens long (see [29]), so the correlation matrix is of dimension 1024×1024 .

¹³Intuitively, multi-head attention heads allow for attending to different parts of the sequence in different ways (i.e. different heads in the multi-head attention layer *attend to* different parts of the input sequence) and can therefore extract richer contextual information.

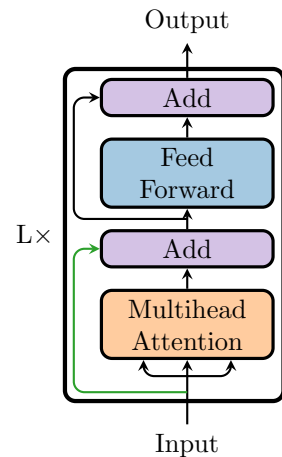


Figure 2: Architecture of a standard transformer.

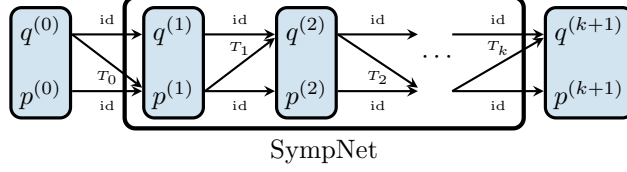


Figure 3: Schematic diagram of a SympNet.

form:

$$\begin{pmatrix} q \\ p \end{pmatrix} \mapsto \begin{pmatrix} q + K^T \text{diag}(a)\sigma(Kp + b) \\ p \end{pmatrix}, \quad \begin{pmatrix} q \\ p \end{pmatrix} \mapsto \begin{pmatrix} q \\ p + K^T \text{diag}(a)\sigma(Kq + b) \end{pmatrix} \quad (7)$$

where K is a $M \times d$ matrix, b and a are vectors of size M and M can be chosen arbitrarily. The name ‘‘gradient layer’’ comes from the fact that the mapping $p \mapsto K^T \text{diag}(a)\sigma(Kp + b)$ can be written as the gradient of a scalar function $p \mapsto a^T \bar{\sigma}(Kp + b) =: g(p)$, where $\bar{\sigma}$ is the antiderivative of the activation function σ . This is easily shown to be symplectic. To see this write $\mathcal{H} = \nabla^2 g$ for the Hessian and further:

$$\begin{pmatrix} \mathbb{I} & \mathcal{H} \\ \mathcal{O} & \mathbb{I} \end{pmatrix} \begin{pmatrix} \mathcal{O} & \mathbb{I} \\ -\mathbb{I} & \mathcal{O} \end{pmatrix} \begin{pmatrix} \mathbb{I} & \mathcal{O} \\ \mathcal{H} & \mathbb{I} \end{pmatrix} = \begin{pmatrix} -\mathcal{H} & \mathbb{I} \\ -\mathbb{I} & \mathcal{O} \end{pmatrix} \begin{pmatrix} \mathbb{I} & \mathcal{O} \\ \mathcal{H} & \mathbb{I} \end{pmatrix} = \begin{pmatrix} \mathcal{O} & \mathbb{I} \\ -\mathbb{I} & \mathcal{O} \end{pmatrix} \quad (8)$$

The transformations in fig. 3 can be alternatively exchanged with the transformations defined in equation 7. The collection of all possible combinations of these layers is referred to as G -SympNets and denoted by Ψ_G . So an element of $\psi \in \Psi_G$ is a composition of gradient layers: $\psi = l_k^G \circ \dots \circ l_0^G$, where k is referred to as the *depth of the SympNet*.

We conclude this section by stating the *universal approximation theorem for SympNets*. Here we denote the set of C^r symplectic maps on an open set $U \subset \mathbb{R}^{2d}$ as:

$$\mathcal{SP}^r(U) := \left\{ \Phi \in C^r(U, \mathbb{R}^{2d}) \mid \left(\frac{\partial \Phi}{\partial x} \right)^T \mathbb{J}_{2d} \left(\frac{\partial \Phi}{\partial x} \right) = \mathbb{J}_{2d} \right\}, \quad r \geq 1$$

Now we state the theorem:

Theorem 3. Ψ_G is r -uniformly dense on compacta in $\mathcal{SP}^r(U)$, where $U \subset \mathbb{R}^{2N}$

This means that $\forall f \in \mathcal{SP}^r(U)$, $K \subset U$ compact and $\epsilon > 0$, $\exists \psi \in \Psi_G$ such that $\|f - \psi\|_{r,K} < \epsilon$ with $\|f\|_{r,K} = \sum_{|\alpha| \leq r} \max_{1 \leq i \leq N} \sup_{x \in K} |D^\alpha f_i(x)|$.

4 Structure-Preserving Attention

In this section we introduce a new attention mechanism that we call *structure-preserving attention*. It treats symplecticity the same way it is defined for a multistep method (see [11]). In order to do so, we first define a notion of symplecticity for the product space¹⁴ $\mathbb{R}^{2d} \times \dots \times \mathbb{R}^{2d} \equiv \times_{T \text{ times}} \mathbb{R}^{2d}$:

$$\tilde{\mathbb{J}}(z^{(1)} \times \dots \times z^{(T)}, \bar{z}^{(1)} \times \dots \times \bar{z}^{(T)}) =: (z^{(1)})^T \mathbb{J}_{2d} \bar{z}^{(1)} + \dots + (z^{(T)})^T \mathbb{J}_{2d} \bar{z}^{(T)}. \quad (9)$$

The two-form $\tilde{\mathbb{J}}: (\times_{(T \text{ times})} \mathbb{R}^{2d}) \times (\times_{(T \text{ times})} \mathbb{R}^{2d}) \rightarrow \mathbb{R}$ is easily seen to be skew-symmetric, linear and non-degenerate¹⁵.

In order to better discuss the symplecticity of the product space $\times_{(T \text{ times})} \mathbb{R}^{2d}$ we define an isomorphism $\times_{(T \text{ times})} \mathbb{R}^{2d} \xrightarrow{\sim} \mathbb{R}^{2dT}$; this way there will not be a difference in the definition of symplecticity to the

¹⁴In section 1 it was discussed that a symplectic vector space is any even-dimensional vector space that is endowed with a distinct non-degenerate skew-symmetric two-form. So we can turn $\mathbb{R}^{2d} \times \dots \times \mathbb{R}^{2d}$ into a symplectic vector space by defining such a form.

¹⁵To proof non-degeneracy we have to show that for any vector $z := z^{(1)} \times \dots \times z^{(T)}, \bar{z}^{(1)} \times \dots \times \bar{z}^{(T)} \neq 0$ on the product space we can find another vector \hat{z} such that $\tilde{\mathbb{J}}(z, \hat{z}) \neq 0$. But we know that at we have at least one integer i for which we can find $\hat{z}^{(i)}$ such that $(z^{(i)})^T \mathbb{J}_{2d} \hat{z}^{(i)} \neq 0$. Now we take for \hat{z} simply $0 \times \dots \times \hat{z}^{(i)} \times \dots \times 0$.

one in section 1. Concretely, the isomorphism $\times_{(T \text{ times})} \mathbb{R}^{2d} \xrightarrow{\sim} \mathbb{R}^{2dT}$ takes the following form:

$$Z = \begin{pmatrix} Q_1 \\ Q_2 \\ P_1 \\ P_2 \\ \vdots \\ p_d^{(1)} \\ p_d^{(2)} \\ \vdots \\ p_d^{(T)} \end{pmatrix} = \begin{bmatrix} q_1^{(1)} & q_1^{(2)} & \cdots & q_1^{(T)} \\ q_2^{(1)} & q_2^{(2)} & \cdots & q_2^{(T)} \\ \vdots & \vdots & \ddots & \vdots \\ q_n^{(1)} & q_n^{(2)} & \cdots & q_n^{(T)} \\ p_1^{(1)} & p_1^{(2)} & \cdots & p_1^{(T)} \\ p_2^{(1)} & p_2^{(2)} & \cdots & p_2^{(T)} \\ \vdots & \vdots & \ddots & \vdots \\ p_d^{(1)} & p_d^{(2)} & \cdots & p_d^{(T)} \end{bmatrix} \mapsto \begin{bmatrix} q_1^{(1)} \\ q_1^{(2)} \\ \vdots \\ q_1^{(T)} \\ q_2^{(1)} \\ \vdots \\ q_d^{(T)} \\ p_1^{(1)} \\ \vdots \\ p_1^{(T)} \\ p_2^{(1)} \\ \vdots \\ p_1^{(T)} \\ p_2^{(1)} \\ \vdots \\ p_d^{(T)} \end{bmatrix} =: Z_{\text{vec}}. \quad (10)$$

The main difficulty in adapting a transformer-like architecture to be symplectic or structure-preserving is to adapt the activation function. Indeed, the softmax acts vector-wise and cannot preserve symplecticity. We thus replace the softmax by a different activation function. This new activation function is a composition of a skew-symmetrization operation Φ and a Cayley transform:

$$\sigma(C) = \text{Cayley}(\Phi(C)), \quad (11)$$

where we have:

$$\Phi_{ij} = \begin{cases} c_{ij} & \text{if } i < j \\ -c_{ji} & \text{if } i > j \\ 0 & \text{else.} \end{cases} \quad \text{and} \quad \text{Cayley}(Y) = \frac{1}{2}(\mathbb{I}_T - Y)(\mathbb{I}_T + Y)^{-1}. \quad (12)$$

The Cayley transform maps skew-symmetric matrices to orthonormal matrices¹⁶, and Φ maps arbitrary matrices to skew-symmetric ones. This results in a new activation function for our attention mechanism which we denote by $\Lambda(Z) = \sigma(Z^T A Z)$. Because $\Lambda(Z)$ is orthonormal the entire mapping is equivalent to a multiplication by a symplectic matrix; in order to see this note that the entire attention layer now does the following:

$$Z \mapsto Z\Lambda(Z), \quad (13)$$

Which is in the transformed coordinate system (with the big vector from eq. (10)) equivalent to a multiplication by a sparse matrix $\tilde{\Lambda}(Z)$ from the left:

$$\tilde{\Lambda}(Z)Z_{\text{vec}} := \begin{pmatrix} \Lambda(Z) & \mathbb{O} & \cdots & \mathbb{O} \\ \mathbb{O} & \Lambda(Z) & \cdots & \mathbb{O} \\ \cdots & \cdots & \ddots & \cdots \\ \mathbb{O} & \mathbb{O} & \cdots & \Lambda(Z) \end{pmatrix} \begin{bmatrix} q_1^{(1)} \\ q_1^{(2)} \\ \vdots \\ q_1^{(T)} \\ q_2^{(1)} \\ \vdots \\ q_d^{(T)} \\ p_1^{(1)} \\ \vdots \\ p_1^{(T)} \\ p_2^{(1)} \\ \vdots \\ p_d^{(T)} \end{bmatrix} \quad (14)$$

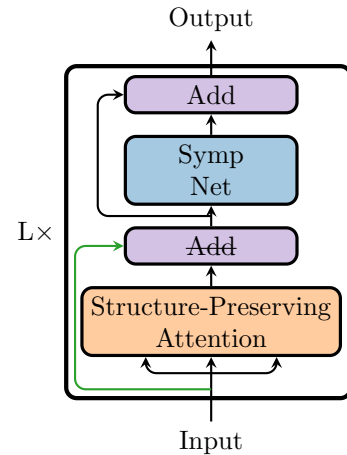


Figure 4: Schematic representation of the structure-preserving transformer.

¹⁶The orthonormal matrices $\{B \in \mathbb{R}^{d \times d} : B^T B = \mathbb{I}_d\}$ form a Lie group under regular matrix multiplication. The associated Lie algebra is the vector space of skew-symmetric matrices $\mathfrak{g} = \{C : C + C^T = 0\}$ and the Lie algebra is mapped to the Lie group via the Cayley transform. More details on this can be found in e.g. [16].

Equation (13) is equivalent to a multiplication by a symplectic matrix if we can show that $\tilde{\Lambda}(Z)^T \mathbb{J}_{2nT} \tilde{\Lambda}(Z) = \mathbb{J}_{2nT}$, where we have defined a big symplectic matrix¹⁷

$$\mathbb{J}_{2dT} = \begin{pmatrix} \mathbb{O} & \mathbb{I}_{dT} \\ -\mathbb{I}_{dT} & \mathbb{O} \end{pmatrix}. \quad (15)$$

Because the matrix $\Lambda(Z)$ is orthonormal, i.e. $\Lambda(Z)^T \Lambda(Z) = \mathbb{I}_T$, the sparse matrix $\tilde{\Lambda}$ is symplectic:

$$(\mathbb{I}_{2d} \otimes \Lambda(Z)^T)(\mathbb{J}_{2d} \otimes \mathbb{I}_T)(\mathbb{I}_{2d} \otimes \Lambda(Z)) = \mathbb{J}_{2d} \otimes (\Lambda(Z)^T \Lambda(Z)) = \mathbb{J}_{2dT}, \quad (16)$$

where we have used tensor product notation, i.e.

$$A \otimes B = \begin{pmatrix} a_{11}B & a_{12}B & \cdots & a_{1n}B \\ a_{21}B & a_{22}B & \cdots & a_{2n}B \\ \cdots & \cdots & \cdots & \cdots \\ a_{d1}B & \cdots & \cdots & a_{dn}B \end{pmatrix}, \quad (17)$$

for a $d \times n$ matrix A .

For the remaining parts of the transformer, the feedforward neural network is replaced by a SympNet and the first add connection is removed, as shown in figure 4. The reason behind removing the add connection is the operations performed by the attention layer would be a multiplication by a symplectic matrix composed with an addition by the input, which would destroy the structure contained in the first operation.

We should also note that the eq. (13) is not perfectly symplectic; even though $\Lambda(Z)$ is a symplectic matrix it still depends on Z and so the Jacobian of this transformation has extra terms. As a result our adapted transformer preserves phase space volume, but is not symplectic in the classical sense, which is a stronger property.

5 Experiments

As a concrete example for a parametrized Hamiltonian system we consider two harmonic oscillators with non-linear coupling:

$$H(q_1, q_2, p_1, p_2) = \frac{p_1^2}{2m_1} + \frac{p_2^2}{2m_2} + k_1 \frac{q_1^2}{2} + k_2 \frac{q_2^2}{2} + k\bar{\sigma}(q_1) \frac{(q_1 - q_2)^2}{2}, \quad (18)$$

with $\bar{\sigma}(x) = 1/(1 + e^{-x})$. For the parameters we choose the following values:

Table 1: Choices for parameter values for the system in eq. (18). Note that all parameters are fixed to one value except k .

m_1	m_2	k_1	k_2	k
2.0	1.0	1.5	0.3	$[0, 4]$

For the training set we pick k to be 40 equally-spaced values in the interval $[0, 4]$ and fix the initial conditions to

$$q(t_0) = \begin{pmatrix} 1 \\ 0 \end{pmatrix} \quad \text{and} \quad p(t_0) = \begin{pmatrix} 2 \\ 0 \end{pmatrix}. \quad (19)$$

Figure 5 shows the coordinate q_1 of solutions of eq. (18) for seven different values for k : 0.00, 0.50, 0.75, 1.00, 2.00, 3.00 and 4.00. The shape of the orbits in fig. 5 changes dramatically depending on what value we pick for k .

We now train four different networks with these data: ResNet, SympNet, transformer and structure-preserving transformer; fig. 6 shows a comparison of these architectures. We use all of these networks to predict the next time steps given an input sequence:

$$\mathcal{NN} : [z^{(t)}, \dots, z^{(t+s1)}] \mapsto [\hat{z}^{(t+s1+1)}, \dots, \hat{z}^{(t+s1+p1)}], \quad (20)$$

¹⁷It can be easily checked that $\tilde{\mathbb{J}}(Z^1, Z^2) = (Z_{\text{vec}}^1)^T \mathbb{J}_{2dT} Z_{\text{vec}}^2$, so the two notions of symplecticity are equivalent.

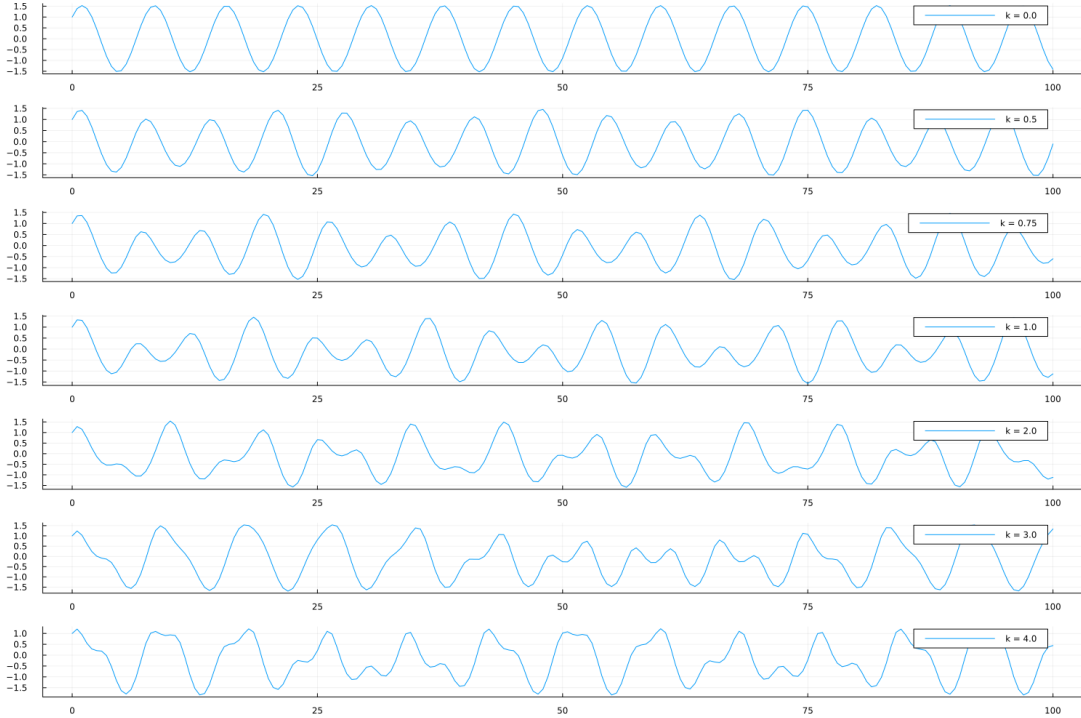


Figure 5: Trajectories coming from eq. (18). The integration is done with implicit midpoint, the time step for the integrator is set to 0.4 and we integrate in the interval $[0, 100]$.

here $\mathbf{s}1$ denotes the *sequence length*, i.e. the length of the sequence that we feed into the network and $\mathbf{p}1$ is the *prediction length*, i.e. the length of the output sequence that is predicted by the network. In theory $\mathbf{p}1$ can be as long as $\mathbf{s}1$ (as a transformer layer always has the same input as output size), but in the experiments here we will set $\mathbf{p}1$ equal to one, i.e. we only take the last column of the output of the transformers for the prediction. This is indicated in fig. 6 by $X \mapsto X[:, \mathbf{end}]$.

The ResNet and the SympNet cannot resolve time series data, which means for both of these $\mathbf{s}1 = \mathbf{p}1 = 1$. These networks only ever *see one vector at a time*.

Note that for all of the architectures shown in fig. 6 also include an *upscaling*. The upscaling maps the low-dimensional input in \mathbb{R}^{2d} to a higher-dimensional space \mathbb{R}^{2N} in which we work with the transformer. For the ResNet and the ordinary transformer the upscaling is done with a simple feedforward neural network, i.e. $x \mapsto \tanh(Ax + b)$ with $A \in \mathbb{R}^{2N \times 2d}$ and $b \in \mathbb{R}^{2N}$. For the SympNet and the structure-preserving transformer the upscaling is done with a *PSD-like layer*. These layers are inspired by proper symplectic decomposition (PSD, see [28]). They have the following form:

$$z \mapsto \begin{pmatrix} \Phi & \mathbb{O} \\ \mathbb{O} & \Phi \end{pmatrix} z, \quad \text{with } \Phi \in St(d, N) \text{ and } \mathbb{O} \in \mathbb{R}^{N \times d}, \quad (21)$$

where $St(d, N)$ is the *Stiefel manifold*, the collection of all $N \times n$ matrices whose columns are in orthonormal relation to each other:

$$St(d, N) := \{\Phi \in \mathbb{R}^{N \times d} : \Phi^T \Phi = \mathbb{I}_d\}. \quad (22)$$

The PSD-like layers in eq. (21) preserve symplecticity, as can be easily shown:

$$\begin{pmatrix} \Phi & \mathbb{O} \\ \mathbb{O} & \Phi \end{pmatrix}^T \mathbb{J}_{2N} \begin{pmatrix} \Phi & \mathbb{O} \\ \mathbb{O} & \Phi \end{pmatrix} = \mathbb{J}_{2d}. \quad (23)$$

Note that the definition of symplecticity here also incorporates that we change dimension with the mapping in eq. (21), i.e. we change the dimension from $2d$ to $2N$. Equation (21) shows the *upscaling layer*; the *downscaling layer* is the same, just with a transpose so that it is a linear layer $\mathbb{R}^{2N} \rightarrow \mathbb{R}^{2d}$.

The ResNets in fig. 6 are simple one-layer feedforward neural networks with add connections $x \mapsto \tanh(Wx + b) + x$ and the SympNets in fig. 6 are compositions of two gradient layers (see

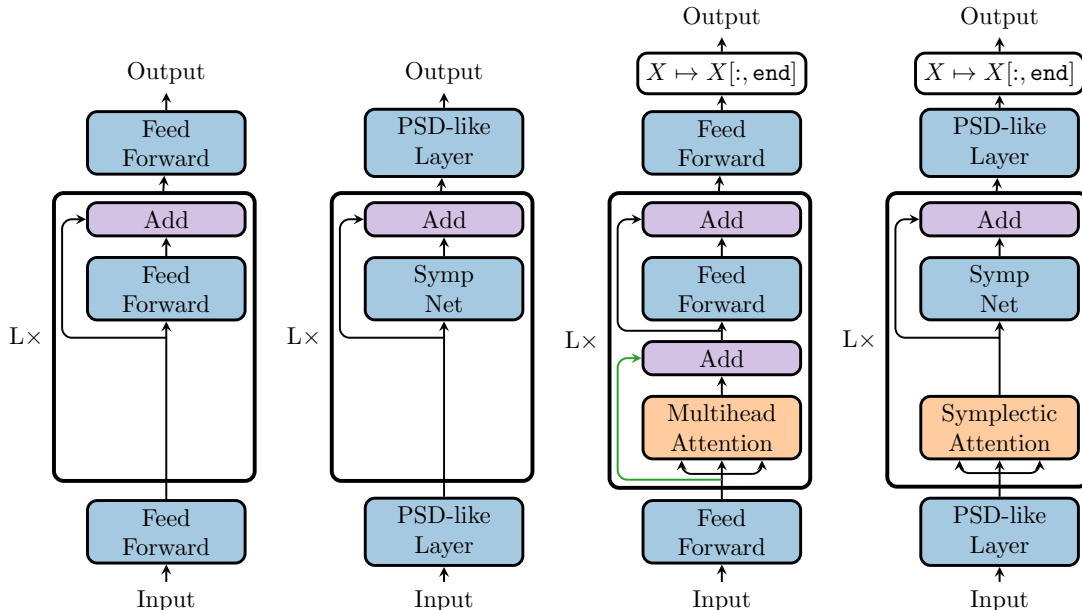


Figure 6: Comparison of the network architectures that we use for integration.

section 3) where the first one changes the q part and the second one changes the p part. The integer M for the gradient layers is chosen to be twice the upscale dimension (i.e. $M = 2N = 40$). Table 2 shows the hyperparameters for our networks (confer fig. 6 and eq. (20)). The hyperparameters for the network architecture are the following: the dimension in which the transformer *operates*, the number of transformer components L , the *number of heads* in the multi-head attention layer¹⁸ $\mathbf{n_heads}$, the sequence length $\mathbf{s1}$ and the length of the output sequence (prediction length) \mathbf{pl} .

Table 2: Choice for hyperparameters in the networks in fig. 6. L is the number of *transformer layers*.

upscale dimension	L	$\mathbf{n_heads}$	$\mathbf{s1}$	\mathbf{pl}
20	2	4	5	1

For training of the different networks we use Adam [22]. For training the networks we again have a set of hyperparameters, shown in table 3.

Table 3: Choice of hyperparameters for the optimization.

η	ρ_1	ρ_2	δ	$\mathbf{n_epochs}$	$\mathbf{batch_size}$
10^{-3}	0.9	0.99	10^{-8}	2000	512

The parameters η , ρ_1 , ρ_2 and δ in table 3 are the learning rate, the first moment, the second moment and a stabilization parameter for the Adam optimizer.

Also note that the structure-preserving transformer now contains some weights that are part of a manifold because of the *PSD-upscaling* and *PSD-downscaling layers* (see fig. 6 and eq. (21)). These layers are trained with the manifold version of Adam introduced in [4].

After having trained the four networks in fig. 6, we test each of them for the case $k = 3.5$; the initial conditions are kept the same as they were for the training data (see eq. (19)). We provide each of them with a sequence of 5 time steps (equivalent to $t = 2.0$ as the time step was chosen as 0.4); these 5 time steps are obtained with implicit midpoint. We start the prediction after this point (i.e. $t = 2.0$).

The coordinate q_1 mapped by the four neural networks are shown in figs. 7a to 7d for the value $k = 3.5$ (note that the trajectory for this value was part of the training set). Figures 7a and 7b show a comparison between ResNet and SympNet up to time $t = 10$ in the first case and $t = 18$ in the second. If we only look at the first ten time steps in fig. 7a it is not immediately clear which of the two networks performs better; they both seem to give a reasonable fit to the data, especially when considering that

¹⁸This is only required for the classical transformer as the structure-preserving one does not use multi-head attention. See [34] for a description of multi-head attention.

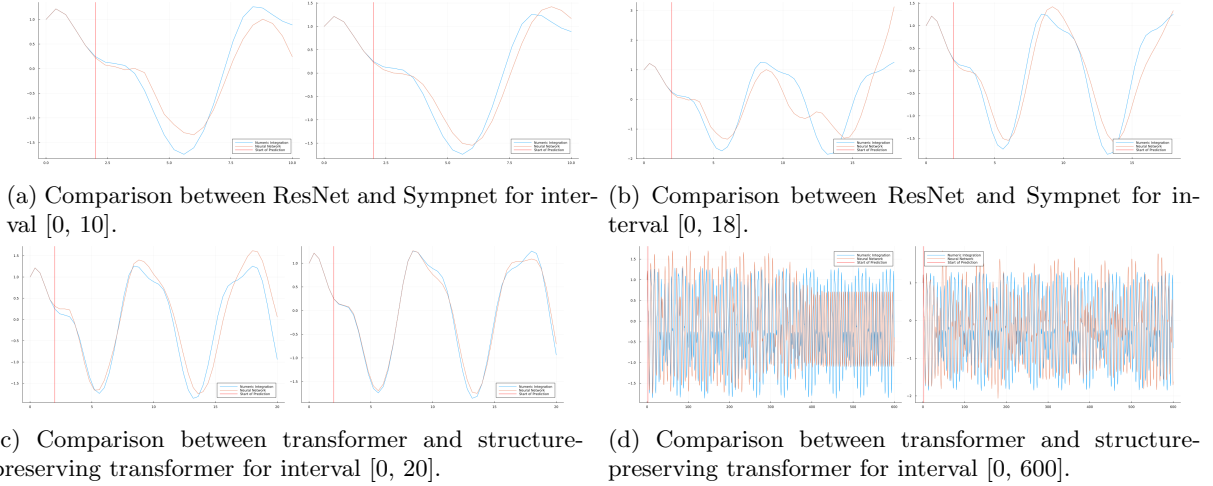


Figure 7: Comparison of SympNet, ResNet, transformer and structure-preserving transformer. The blue line is numerical integration (with implicit midpoint) and the orange one is the neural network integrator.

they cannot resolve parameter dependence. But looking at the system at time step 18 in fig. 7b the advantage of the SympNet over the ResNet becomes obvious: the ResNet was trained to minimize errors for a single time step but has no notion of symplecticity or other long-term stability encoded in it. This leads to the trajectory quickly blowing up as soon as it sees input data that only mildly differs from the training data.

The SympNet however still suffers from the other problem previously discussed: as the ResNet and the SympNet both cannot process time series data, they will yield the similar trajectories regardless of the parameter k that we use to simulate the first five data points. The transformer and the structure-preserving transformer, in particular the latter, show a much better fit to the data in fig. 7c. Considering that we supplied the networks with only five time steps, the transformers can fit the data remarkably well.

In fig. 7d we can see that the classical transformer (without any structure-preserving properties) eventually becomes unstable and seems to loose energy. For the new structure-preserving tranformer this is not the case: the trajectories evolve on paths that may diverge from the numerical solution, but still seem to keep the same energy levels.

6 Conclusion

We have introduced a new neural network architecture for learning the dynamics of Hamiltonian systems. We call this new architecture structure-preserving transformer. It is based on the classical transformer, but modifies the attention mechanism such that it respects the Hamiltonian nature of the system it is applied to. We have shown superior long-term behaviour of the new network when compared to the classical transformer, while also demonstrating that it can resolve time series data.

Acknowledgements

We would like to thank the Centre International de Rencontres Mathématiques (CIRM) for their excellent hospitality that made this project possible.

We further thank all participants of the Cemracs 2023 hackathon with who we had stimulating and helpful discussions.

References

- [1] V. I. Arnold. Mathematical Methods of Classical Mechanics. Graduate Texts in Mathematics. Springer, New York City, 1978.

- [2] Nathan Baker, Frank Alexander, Timo Bremer, Aric Hagberg, Yannis Kevrekidis, Habib Najm, Manish Parashar, Abani Patra, James Sethian, Stefan Wild, et al. Workshop report on basic research needs for scientific machine learning: Core technologies for artificial intelligence. Technical report, USDOE Office of Science (SC), Washington, DC, 2019.
- [3] Richard L Bishop and Samuel I Goldberg. Tensor Analysis on Manifolds. Dover Publications, Mineola, NY, 1980.
- [4] Benedikt Brantner. Generalizing adam to manifolds for efficiently training transformers. arXiv preprint arXiv:2305.16901, 2023.
- [5] Benedikt Brantner and Michael Kraus. Symplectic autoencoders for model reduction of hamiltonian systems. arXiv preprint arXiv:2312.10004, 2023.
- [6] Patrick Buchfink, Silke Glas, and Bernard Haasdonk. Symplectic model reduction of hamiltonian systems on nonlinear manifolds and approximation with weakly symplectic autoencoder. SIAM Journal on Scientific Computing, 45(2):A289–A311, 2023.
- [7] Saifon Chaturantabut and Danny C Sorensen. Nonlinear model reduction via discrete empirical interpolation. SIAM Journal on Scientific Computing, 32(5):2737–2764, 2010.
- [8] Boyuan Chen, Kuang Huang, Sunand Raghupathi, Ishaan Chandratreya, Qiang Du, and Hod Lipson. Discovering state variables hidden in experimental data. arXiv preprint arXiv:2112.10755, 2021.
- [9] Germund Dahlquist. Error analysis for a class of methods for stiff non-linear initial value problems. Numerical Analysis, pages 60–72, 1976.
- [10] Alexey Dosovitskiy, Lucas Beyer, Alexander Kolesnikov, Dirk Weissenborn, Xiaohua Zhai, Thomas Unterthiner, Mostafa Dehghani, Matthias Minderer, Georg Heigold, Sylvain Gelly, et al. An image is worth 16x16 words: Transformers for image recognition at scale. arXiv preprint arXiv:2010.11929, 2020.
- [11] Kang Feng. The step-transition operators for multi-step methods of ode’s. Journal of Computational Mathematics, pages 193–202, 1998.
- [12] Kang Feng. The step-transition operators for multi-step methods of ode’s. Journal of Computational Mathematics, 16(3):193–202, 1998.
- [13] Stefania Fresca, Luca Dede, and Andrea Manzoni. A comprehensive deep learning-based approach to reduced order modeling of nonlinear time-dependent parametrized pdes. Journal of Scientific Computing, 87(2):1–36, 2021.
- [14] Pawan Goyal and Peter Benner. Lqresnet: a deep neural network architecture for learning dynamic processes. arXiv preprint arXiv:2103.02249, 2021.
- [15] Alex Graves and Alex Graves. Long short-term memory. Supervised sequence labelling with recurrent neural networks, pages 37–45, 2012.
- [16] Ernst Hairer, Christian Lubich, and Gerhard Wanner. Geometric Numerical integration: structure-preserving algorithms for ordinary differential equations. Springer, Heidelberg, 2006.
- [17] Kaiming He, Xiangyu Zhang, Shaoqing Ren, and Jian Sun. Deep residual learning for image recognition. In Proceedings of the IEEE conference on computer vision and pattern recognition, pages 770–778, 2016.
- [18] AmirPouya Hemmasian and Amir Barati Farimani. Reduced-order modeling of fluid flows with transformers. Physics of Fluids, 35(5), 2023.
- [19] Sepp Hochreiter and Jürgen Schmidhuber. Long short-term memory. Neural computation, 9(8):1735–1780, 1997.
- [20] Kurt Hornik, Maxwell Stinchcombe, and Halbert White. Multilayer feedforward networks are universal approximators. Neural networks, 2(5):359–366, 1989.

- [21] Pengzhan Jin, Zhen Zhang, Aiqing Zhu, Yifa Tang, and George Em Karniadakis. Sympnets: Intrinsic structure-preserving symplectic networks for identifying hamiltonian systems. Neural Networks, 132:166–179, 2020.
- [22] Diederik P Kingma and Jimmy Ba. Adam: A method for stochastic optimization. arXiv preprint arXiv:1412.6980, 2014.
- [23] Michael Kraus. Variational integrators in plasma physics. arXiv preprint arXiv:1307.5665, 2013.
- [24] Serge Lang. Algebra, volume 211. Springer-Verlag, Heidelberg, 2012.
- [25] Toni Lassila, Andrea Manzoni, Alfio Quarteroni, and Gianluigi Rozza. Model order reduction in fluid dynamics: challenges and perspectives. Reduced Order Methods for modeling and computational reduction, pages 235–273, 2014.
- [26] Kookjin Lee and Kevin T Carlberg. Model reduction of dynamical systems on nonlinear manifolds using deep convolutional autoencoders. Journal of Computational Physics, 404:108973, 2020.
- [27] Benedict Leimkuhler and Sebastian Reich. Simulating hamiltonian dynamics. Cambridge university press, Cambridge, UK, 2004.
- [28] Liqian Peng and Kamran Mohseni. Symplectic model reduction of hamiltonian systems. SIAM Journal on Scientific Computing, 38(1):A1–A27, 2016.
- [29] Alec Radford, Jeffrey Wu, Rewon Child, David Luan, Dario Amodei, Ilya Sutskever, et al. Language models are unsupervised multitask learners. OpenAI blog, 1(8):9, 2019.
- [30] Maziar Raissi, Paris Perdikaris, and George E Karniadakis. Physics-informed neural networks: A deep learning framework for solving forward and inverse problems involving nonlinear partial differential equations. Journal of Computational physics, 378:686–707, 2019.
- [31] David E Rumelhart, Geoffrey E Hinton, Ronald J Williams, et al. Learning internal representations by error propagation, 1985.
- [32] Alberto Solera-Rico, Carlos Sanmiguel Vila, MA Gómez, Yuning Wang, Abdulrahman Almashjary, Scott Dawson, and Ricardo Vinuesa. β -variational autoencoders and transformers for reduced-order modelling of fluid flows. arXiv preprint arXiv:2304.03571, 2023.
- [33] Tomasz M Tyranowski and Michael Kraus. Symplectic model reduction methods for the vlasov equation. Contributions to Plasma Physics, 2022.
- [34] Ashish Vaswani, Noam Shazeer, Niki Parmar, Jakob Uszkoreit, Llion Jones, Aidan N Gomez, Lukasz Kaiser, and Illia Polosukhin. Attention is all you need. Advances in neural information processing systems, 30, 2017.